Colloids and Surfaces B: Biointerfaces 128 (2015) 140–148

Contents lists available at ScienceDirect

Colloids and Surfaces B: Biointerfaces

journal homepage: www.elsevier.com/locate/colsurfb

Dextran-based hydrogel formed by thiol-Michael addition reaction for 3D cell encapsulation

Zhen Qi Liu[a,b], Zhao Wei[a,b], Xv Long Zhu[c,d], Guo You Huang[b,e], Feng Xu[b,e], Jian Hai Yang[a,b], Yoshihito Osada[f], Miklós Zrínyi[g], Jian Hui Li[d,*], Yong Mei Chen[a,b,**]

[a] School of Science, State Key Laboratory for Mechanical Behaviour of Materials, Collaborative Innovation Center of Suzhou Nano Science and Technology, Xi'an Jiaotong University, Xi'an 710049, China
[b] Bioinspired Engineering and Biomechanics Center (BEBC), Xi'an Jiaotong University, Xi'an 710049, China
[c] School of Medicine, Yan'an University, Yan'an 716000, China
[d] Department of Surgical Oncology, Shaanxi Provincial People's Hospital, Xi'an 710068, China
[e] The Key Laboratory of Biomedical Information Engineering of Ministry of Education, School of Life Science and Technology, Xi'an Jiaotong University, Xi'an 710049, China
[f] RIKEN 2-1, Hirosawa, Wako, Saitama 351-0198, Japan
[g] Laboratory of Nanochemistry, Department of Biophysics and Radiation Biology, Semmelweis University, H-1084 Budapest, Nagyvárad tér 4, Hungary

ARTICLE INFO

Article history:
Received 31 August 2014
Received in revised form 31 January 2015
Accepted 2 February 2015
Available online 9 February 2015

Keywords:
Hydrogel
Thiol-Michael addition
Dextran
3D cell encapsulation
Bone marrow mesenchymal stem cells

ABSTRACT

Cell encapsulation in three-dimensional (3D) hydrogels can mimic native cell microenvironment and plays a major role in cell-based transplantation therapies. In this contribution, a novel in situ-forming hydrogel, Dex-l-DTT hydrogel ("l" means "linked-by"), by cross-linking glycidyl methacrylate derivatized dextran (Dex-GMA) and dithiothreitol (DTT) under physiological conditions, has been developed using thiol-Michael addition reaction. The mechanical properties, gelation process and degree of swelling of the hydrogel can be easily adjusted by changing the pH of phosphate buffer saline. The 3D cell encapsulation ability is demonstrated by encapsulating rat bone marrow mesenchymal stem cells (BMSCs) and NIH/3T3 fibroblasts into the in situ-forming hydrogel with maintained high viability. The BMSCs also maintain their differentiation potential after encapsulation. These results demonstrate that the Dex-l-DTT hydrogel holds great potential for biomedical field.

1. Introduction

Three-dimensional (3D) cell culture systems find widespread applications in biomedical field, due to their capability of mimicking the native microenvironment necessary for cell–cell and cell–matrix interactions [1,2]. Various 3D culture systems have been developed, such as cell spheroids for studying tumor behaviors [3,4], microcarrier culture for proliferating stem cell [5–7], tissue-engineered scaffolds for modeling bone marrow niches [8] and cell encapsulation for cell-based transplantation therapies [9–11]. Among these 3D systems, encapsulating cells into suitable scaffolds has attracted increasing attention due to some advantages, including ease of handling, highly hydrated tissue-like microenvironment and uniform cell distribution [12–14].

Hydrogel, a representative soft and wet biomaterial with tunable properties mimicing native extracellular matrix (ECM), such as high water content, excellent mass transportation and tissue-like elasticity [15,16], is one of the most promising soft biomaterials for 3D cell encapsulation [12,17,18]. Various hydrogels have been used for 3D cell encapsulation, including natural-derived hydrogels (e.g., Matrigel™ [19], collagen [20,21], and fibrin [22]), as well as synthetic hydrogels (e.g., polyethylene glycol (PEG) [23–27], polyvinyl alcohol (PVA) [28], and polyhydroxyethyl methacrylate (PHEMA) [29]). Although natural-derived hydrogels have excellent biocompatibility, the disadvantages of high batch-to-batch variations, undefined matrix compositions and restricted modification possibilities [1,30] significantly limit their applications. By contrast, synthetic hydrogels have defined chemical structures and stable physicochemical properties [31–33]. Unfortunately, they involve the biocompatibility issue since they lack the biologically relevant chemistries [30], and are considered as foreign object for cells. Therefore, there is still an unmet need of hydrogels with good

* Corresponding author.
** Corresponding author at: School of Science, State Key Laboratory for Mechanical Behaviour of Materials, Collaborative Innovation Center of Suzhou Nano Science and Technology, Xi'an Jiaotong University, Xi'an 710049, China. Tel.: +86 29 82663914; fax: +86 29 82668559.
E-mail address: chenym@mail.xjtu.edu.cn (Y.M. Chen).

http://dx.doi.org/10.1016/j.colsurfb.2015.02.005
0927-7765/

biocompatibility and easy modification for designing diverse 3D cell encapsulation systems.

To address above challenge, semi-synthetic hydrogels combining both the advantages of natural-derived and synthetic hydrogels have been proposed. As popular biomaterials, hyaluronic acid and alginate have been abundantly reported to prepare semi-synthetic hydrogels for 3D cell encapsulation in the past decades [34–36]. Exploring novel hydrogel system for 3D cell encapsulation will arouse a general readership among the scientists in the fields of biomaterial, in particular researchers working on 3D cell encapsulation. As a natural-derived polysaccharide constituted by glucose, dextran has attracted wide attention as excellent biomacromolecule for preparing semi-synthetic hydrogels, owing to the properties of biocompatibility, nontoxicity and easy chemical modification [37–39]. Although several dextran-based semi-synthetic hydrogels have been investigated for drug delivery, protein release and biosensor [40–42], there are few reports on 3D cell encapsulation system due to the lack of appropriate gelation approach.

Among various hydrogels prepared by different procedures, in situ-forming hydrogels, which can directly encapsulate cells in the process of gelation, have been extensively explored as scaffolds for 3D cell encapsulation, due to many favorable characteristics, including homogenous encapsulation of cells and moldability of complex shapes [43,44]. However, the existing in situ gelation approaches involve cell toxicity derived from some chemicals (e.g., monomer, initiator) or gelation procedures (e.g., UV light, heating) [30,45]. Thiol-Michael addition reaction, a highly regioselective and efficient click chemistry reaction, holds great potential to address these challenges [46]. Additionally, the reaction can be carried out under physiological conditions, making them compelling reactions within the bioengineering toolkit for fabricating 3D hydrogel scaffolds [37,38,47].

In this contribution, we designed an in situ-forming dextran-based hydrogel for 3D cell encapsulation via nontoxic gelation procedure under physiological conditions. The glycidyl methacrylate derivatized dextran (Dex-GMA)-based hydrogel cross-linked by dithiothreitol (DTT) can be facilely prepared by mixing Dex-GMA and DTT dissolved in phosphate buffer saline (PBS). Two kinds of cells, rat bone marrow mesenchymal stem cells (BMSCs) and NIH/3T3 fibroblasts have been successfully encapsulated into the semi-synthetic hydrogel. More than 90% cells encapsulated in the system survived, and the BMSCs maintained their differentiation potential.

2. Materials and methods

2.1. Synthesis and characterization of Dex-GMA

Synthesis of GMA-modified dextran derivatives (Dex-GMA) was conducted as previously described [48]. In a typical reaction, Dextran (M_w = 40,000) (10 g, 62 mmol glucopyranosyl ring) was dissolved in 40 mL of DMSO and the solution was stirred for 1 h under nitrogen. After the dextran was completely dissolved and the solution became transparent, 1.9 g 4-dimethylaminopyridine (DMAP) (15.5 mmol) and 4.4 g glycidyl methacrylate (GMA, 31 mmol) were added to the solution. Then the solution was stirred at 50 °C for another 12 h and after that, an equimolar amount of HCl was added to the mixture to neutralize the DMAP. When the reaction finished, the mixture was transferred into dialysis bag (M_w cutoff 8 kDa) to dialyze against distilled water for one week. At last, water was removed by lyophilization to obtain Dex-GMA derivatives as a white fluffy product. The degree of substitution (DS) was determined from ^{1}H NMR spectra by comparing the ratio of the areas under the proton peaks at 6.18 ppm to the peak at 4.94 ppm (Fig. S1). ^{1}H NMR spectra were recorded in D_2O on a 400 MHz NMR spectrometer (Bruker, Switzerland).

2.2. Rheological characterization

The kinetics of gel formation was evaluated using the rheometer equipped with a 50 mm, 1° cone (MCR302, Anton Paar, Austria). Briefly, 10 wt% Dex-GMA and stoichiometric equivalent DTT (1.36 wt%) in phosphate buffer saline (PBS) were put into the gap between lower plate and cone, and the temperature was kept at 37 °C. During the hydrogel formation process, the storage modulus (G') and loss modulus (G'') were monitored for 60 min under a condition of 10 rad/s shear rate and 10% strain.

2.3. Young's modulus evaluation

The Young's modulus of the hydrogel was evaluated by compressive stress–strain measurements using a tensile-compressive tester (CMT6503, MTS, USA). The hydrogels equilibrated in PBS with different pH were punched into disk-shaped samples (15 mm diameter, 2–3 mm thickness) by a hole punch. Then the samples were compressed at a strain rate of 10% min^{-1} at room temperature. The Young's modulus was determined by the average slope of stress–strain curve in the strain range of 0.05–0.1, and each value was averaged over four parallel measurements.

2.4. Degree of swelling and swelling volume ratio

The degree of swelling of the hydrogels was obtained by soaking the hydrogels in PBS with different pH until they reached the equilibrium state. The degree of swelling of hydrogel was quantified as the weight ratio of the swollen state (W_s) of hydrogel to that in the dry state (W_d), that is, degree of swelling = W_s/W_d. The swelling volume ratio of hydrogel was quantified as volume ratio of the swollen state (V) of hydrogel to that in the initial state (V_0), that is, swelling volume ratio = V/V_0.

2.5. Cytotoxicity

MTT assay was conducted to evaluate the cytotoxicity of Dex-GMA and DTT. Briefly, 200 μL NIH/3T3 fibroblasts (ATCC, Manassas, USA) or BMSCs suspension with a density of 5×10^4 cell/mL was seeded to 96-well tissue culture polystyrene (TCPS) and then were cultured for 24 h. The culture medium was discarded after 24 h and the medium containing Dex-GMA or DTT was added into the TCPS. The concentration of Dex-GMA or DTT was 0, 0.5, 1, 1.5, and 2.0 mg/mL. After treatment by Dex-GMA or DTT for interesting time (24, 48 h), the medium was discarded and fresh culture medium containing 0.5 mg/mL MTT was added to each well. The plate was then incubated for 4 h. After incubation, the medium containing MTT was discarded and dimethyl sulfoxide (DMSO) was added. Then the plate containing samples was measured in a microplate reader at 490 nm (Thermo Scientific Multiskan GO, USA). Every experiment was repeated for three times.

2.6. 3D cell encapsulation

The 3D cell encapsulation using in situ-forming Dex-l-DTT hydrogel was conducted according to the following procedures. DMEM/HIGHGLUCOSE (Thermo Fisher Scientific, USA) containing 10% (v/v) fetal bovine serum (Invitrogen, Carlsbad, CA, USA), 100 U/mL penicillin, 100 U/mL streptomycin (Invitrogen, Carlsbad, CA, USA) and α-MEM (Sigma–Aldrich, China) containing 10% (v/v) fetal bovine serum (Invitrogen, Carlsbad, CA, USA), 100 U/mL penicillin, 100 U/mL streptomycin (Invitrogen, Carlsbad, CA, USA) was used for NIH/3T3 fibroblasts and BMSCs culture, respectively. BMSCs used here was prepared following the previous literature [49]. The cells (NIH/3T3 fibroblasts or BMSCs) with a density of

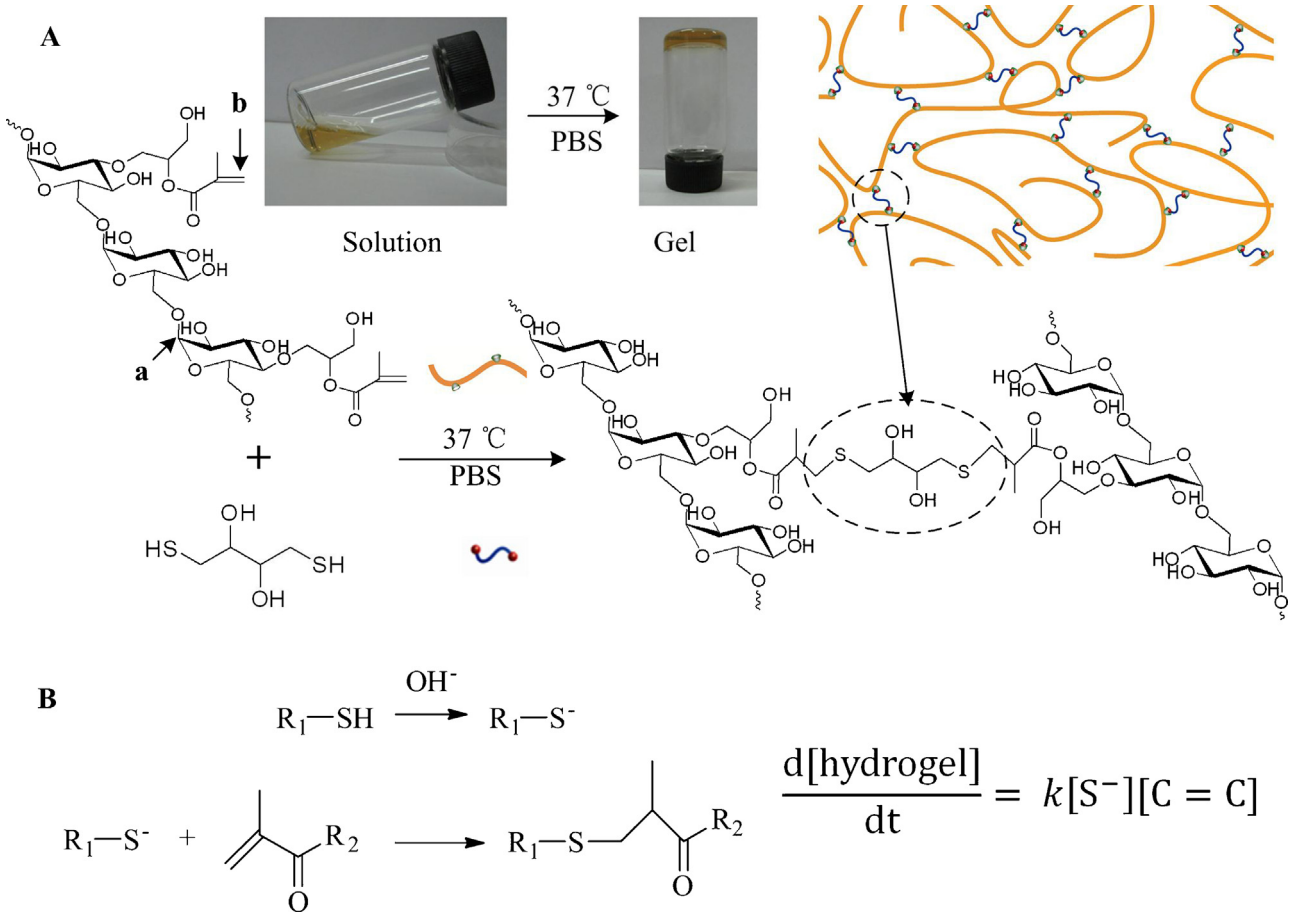

Fig. 1. Overview of Dex-l-DTT hydrogel formation by thiol-Michael addition click reaction. (A) Schematic representation of the formation of the hydrogels and digital photos of the gelation process. (B) The reaction mechanism and reaction rate equation of the thiol-Michael addition reaction used in the hydrogel formation.

3×10^6 cell/mL were mixed with culture medium containing stoichiometric equivalent Dex-GMA (10 wt%) and DTT (1.36 wt%). Then, the cell suspension was transferred to 24-well TCPS and allowed to complete gelation process within 5 min. After the cell-encapsulated hydrogel formed, they were transferred to 6-well TCPS for cultivation at 37 °C with 5% CO_2. At the initial 24 h, medium was changed every 6 h, and after that the medium was changed every 24 h.

2.7. Cell viability

Cell viability was assessed with LIVE/DEAD Viability/Cytotoxicity Kit containing Calcein acetoxymethyl ester (Calcein AM) and Ethidium Homodimer 1 (EthD-1) (Molecular Probes, USA) and MTT assay. At the time point of interest, a portion of cell-encapsulated hydrogel was incubated in 200 μL working solution containing 2 μM Calcein AM and 4 μM EthD-1 for 25 min, and then the hydrogel was rinsed with PBS. The images of the cells were visualized with fluorescence microscopy (OLYMPUS, Tokyo, Japan), and the numbers of live and dead cells were quantified using Image Pro Plus 6.0. When MTT assay was used to detect cell viability, the procedure was performed as follows. Cell-encapsulated hydrogel was punched into disk-shaped samples (with diameter of 4 mm and thickness of 2 mm) and these samples were transferred into 96-well TCPS. At the initial 24 h, culture medium was changed every 6 h, and after that the culture medium was changed every 24 h. At the time point of interest, the medium was discarded and fresh culture medium containing 0.5 mg/mL MTT was added to each well. The plate was then incubated for 4 h. After incubation, the medium containing MTT was discarded and DMSO was added. Then the plate containing samples was measured in a microplate reader at 490 nm (Thermo Scientific Multiskan GO, USA). Every experiment was repeated for three times.

2.8. ALP activity assay

ALP activity was measured using the ALP kit (Nanjing Jian Cheng Bioengineering Institute, China) according to the manufacturer's instruction [50]. Briefly, the BMSCs-encapsulated hydrogels were first cultured in α-MEM medium containing 10% FBS for 24 h and then the medium were changed to osteogenic induction medium (α-MEM was supplemented with 10% FBS, 10 mM β-glycerol phosphate (Sigma), 50 μg/mL ascorbate-2-phosphate (Sigma) and 10^{-7} M dexamethasone (Sigma)). BMSCs-encapsulated hydrogel cultured in α-MEM medium containing 10% FBS (without β-glycerol phosphate, ascorbate-2-phosphate and dexamethasone) was used as control group. On day 1, 3, 5, 7, 9, and 14 of cultivation, a portion of hydrogel with the same volume were punched from the samples and rinsed by PBS for three times. Then, the hydrogel was immersed into 250 μL RIPA Lysis Buffer overnight at 4 °C to collect the supernatant liquid to test the ALP activity during the osteogenesis process.

3. Results and discussion

3.1. Hydrogel synthesis

Dextran modified by glycidyl methacrylate (Dex-GMA) was synthesized by the coupling reaction of dextran (M_w = 40,000) and

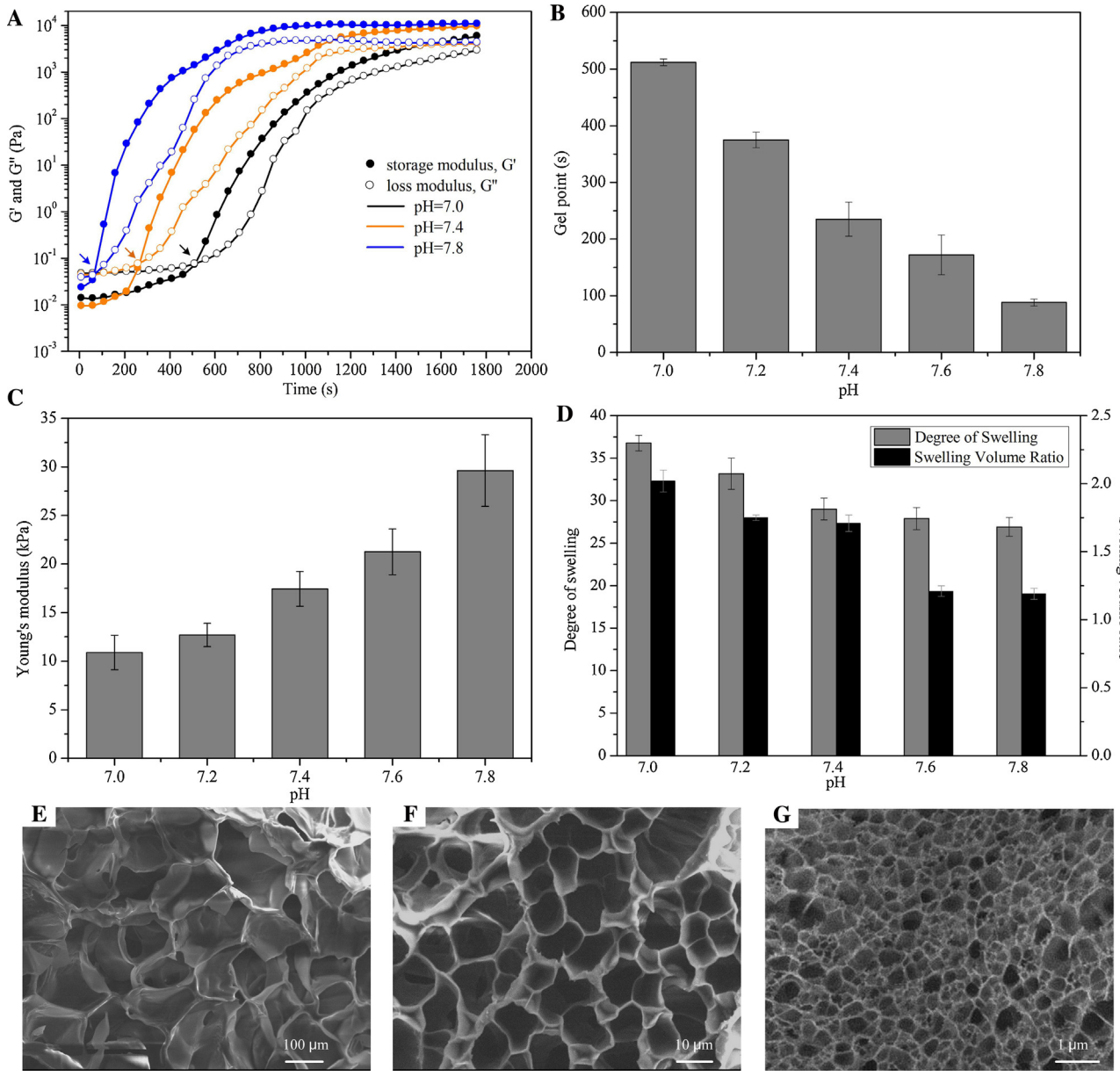

Fig. 2. The effect of pH on the gelation process and properties of Dex-l-DTT hydrogel. (A) Rheology analysis of the gelation process. The storage modulus G' (solid) and loss modulus G'' (hollow) of the system during the gelation process under pH = 7.0 (black), pH = 7.4 (orange) and pH = 7.8 (blue). The arrow indicated the crossover point of G' and G''. (B) Gel point obtained from the rheology analysis. (C) The Young's modulus of hydrogels formed with different pH PBS. (D) Degree of swelling and swelling volume ratio of hydrogels formed with different pH PBS. SEM image of the surface texture of hydrogels prepared in PBS under (E) pH = 7.0, scale bar: 100 μm, (F) pH = 7.4, scale bar: 10 μm, (G) pH = 7.8, scale bar: 1 μm. Error ranges are standard deviations over $n = 4$ samples. (For interpretation of the references to color in this figure legend, the reader is referred to the web version of the article.)

glycidyl methacrylate (GMA) in dimethyl sulfoxide (DMSO) following the literature procedures [48]. The degree of substitution (DS) of dextran was calculated by comparing the integral of signals at $\delta = 6.18$ (Hb) and 4.94 (Ha) according to NMR spectra (Figs. 1A and S1). Herein, the DS of dextran was 37%, and Dex-GMA concentration was set at 10 wt%. When the concentration of Dex-GMA is lower than 10 wt%, the gelation process is very slow or cannot occur, while the Dex-GMA cannot be completely dissolved in PBS when Dex-GMA concentration is higher than 10 wt%.

The in situ-forming Dex-l-DTT ("l" means "linked-by") hydrogel can be easily prepared by simply mixing Dex-GMA and DTT in PBS, via thiol-Michael reaction between methyl acrylate (from Dex-GMA) and thiol (from DTT) groups under physiological temperature (37 °C). The gelation process of Dex-l-DTT hydrogel can be confirmed through vial tilting method. Once homogeneously mixing DTT solution with Dex-GMA solution (brownish yellow color originated from carbonyl group contained in ester bond) at the same molar ratio of the functional groups ($R = M_{MA}:M_{thiol}$, $R = 1$) under physiological conditions, the fluidity of the reaction mixture gradually decreased, and the Dex-l-DTT hydrogel could be obtained within a few minutes (Fig. 1A).

3.2. Effect of pH on hydrogel properties

According to the reaction mechanism, thiols can be easily deprotonated in an alkaline pH and become Michael acceptors, thiol anion (S^-), which readily reacts with certain electron-deficient double bonds (Fig. 1B). Thus, the Dex-l-DTT hydrogel formation can

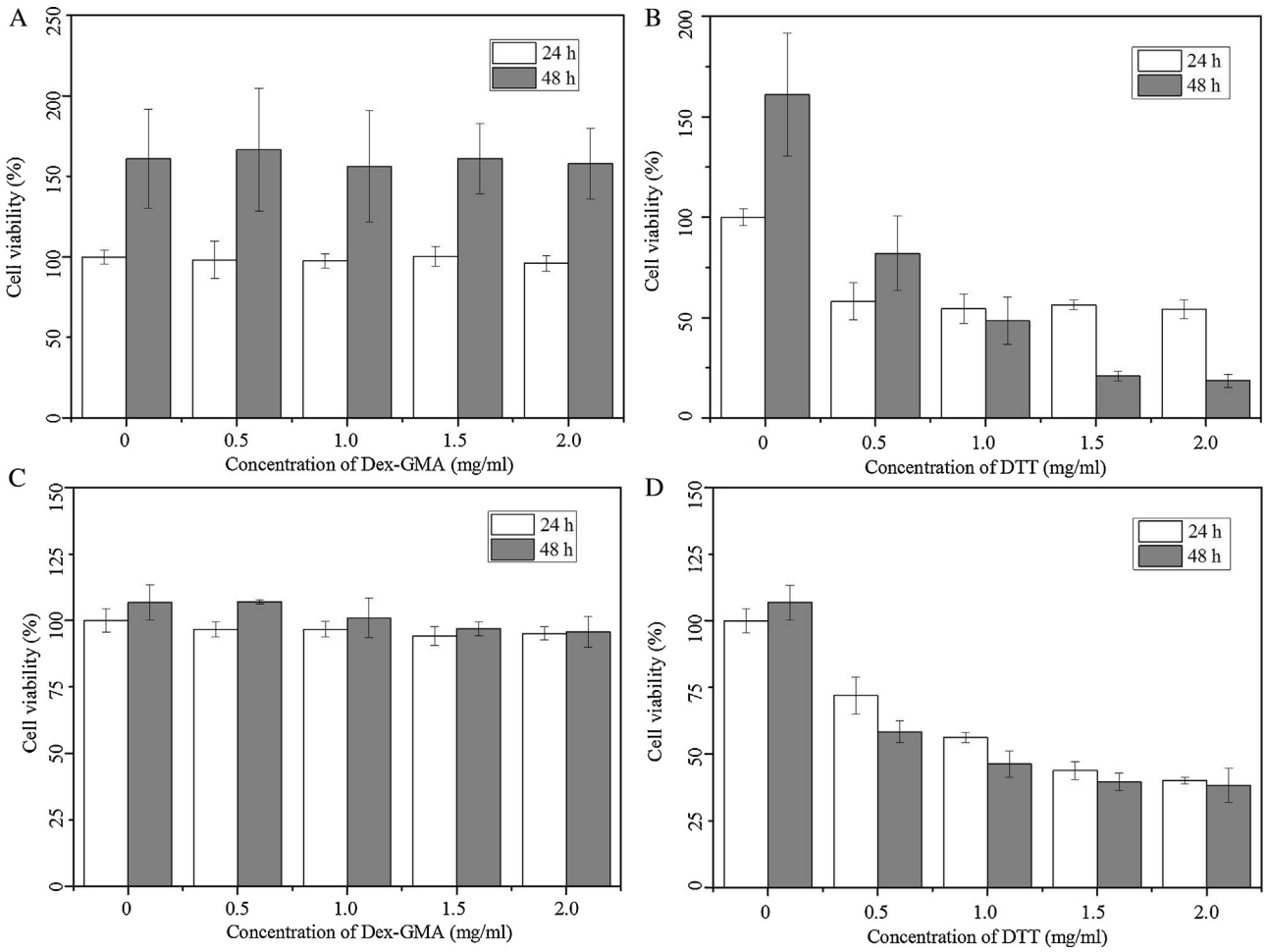

Fig. 3. The cytotoxicity of Dex-GMA and DTT tested by MTT assay over 24 h and 48 h. Viability of NIH/3T3 fibroblasts cultured in medium containing Dex-GMA (A) and DTT (B) with different concentrations. Viability of BMSCs cultured in medium containing Dex-GMA (C) and DTT (D) with different concentrations. Error ranges are standard deviations over $n = 4$ samples.

be controlled by two parameters: pH, which determines the concentration of thiol anion (S^-), and the molar ratio of methyl acrylate to thiol (R). When R was set as a constant ($R = 1$), pH would be the key parameter to control the in situ gelation process. Therefore, we designed a series of experiments to study the effect of pH on the hydrogel properties. All the following experiments were tested while keeping $R = 1$.

To assess the mechanical properties in the process of the in situ gelation of Dex-l-DTT hydrogel, we performed rheology test (Fig. 2A and B). The crossover point of storage modulus (G') and loss modulus (G'') marks the transition from liquid-like to solid-like behavior, which is often used as an estimation of gel point (Fig. 2A) [51]. As the pH was increased from 7.0 to 7.8, the gelation rate increased as demonstrated by earlier gel point (short gelling time, Fig. 2B). For example, the hydrogel reached the gel point within 88 ± 5 s in pH = 7.8 PBS which was approximately 6-fold faster than that in pH = 7.0 PBS (gel point 512 ± 6 s). The results indicate that the in situ gelation process can be accelerated by increasing pH, which is coincident with the proposed reaction scheme (Fig. 1B). On the other hand, these results also demonstrate that the Dex-l-DTT hydrogel is stable with pH ranging from 7.0 to 7.8, which is the range applicable for biomedical applications [23].

Besides gel point, the hydrogel properties including Young's modulus, degree of swelling, swelling volume ratio and morphology of surface texture, were also affected by pH. The Young's modulus of the hydrogel prepared under pH = 7.8 was 29.6 ± 3.7 kPa, which is higher than that prepared under pH = 7.0 (10.9 ± 1.8 kPa) (Fig. 2C). As demonstrated by reaction mechanism, high pH enhances reaction rate between methyl acrylate and thiol groups, therefore, nearly all the function groups can be activated at the same time and participate in the thiol-Michael addition reaction, resulting in densely cross-linked hydrogel with high Young's modulus. However, when the pH is decreased, only part of the

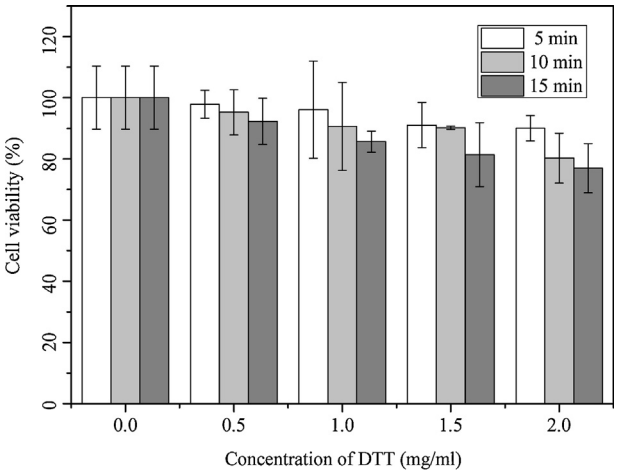

Fig. 4. Viability of NIH/3T3 fibroblasts cultured in medium containing DTT with different concentrations for 5 min, 10 min, and 15 min. Error ranges are standard deviations over $n = 4$ samples.

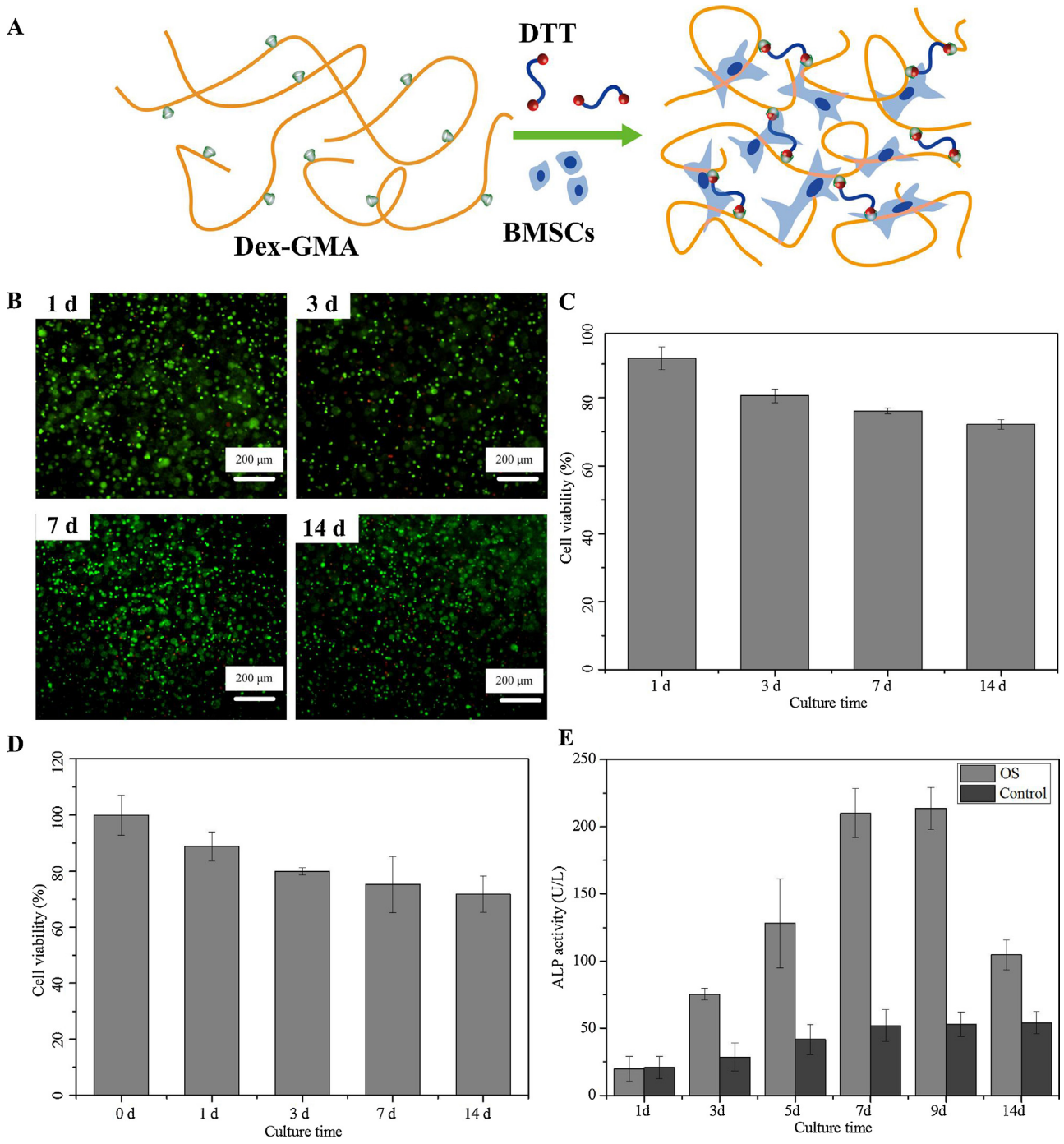

Fig. 5. Viability and differentiation potential of BMSCs encapsulated in Dex-l-DTT hydrogel. (A) Schematic representation of cell encapsulation processes. (B) Live/dead images of BMSCs encapsulated in the hydrogel for 1 d, 3 d, 7 d, and 14 d. Green fluorescence designates live cells, whereas red fluorescence indicates dead cells. (C) Cell viability obtained from the fluorescent images. (D) Cell viability of encapsulated BMSCs detected by MTT assay. (E) The ALP activity of encapsulated BMSCs cultured in osteogenic induction medium (OS) and normal medium (Control) for 1 day to 14 days. Error ranges are standard deviations over $n = 4$ samples. (For interpretation of the references to color in this figure legend, the reader is referred to the web version of the article.)

function groups can react with each other and form defective polymer networks, resulting in loosely cross-linked hydrogel and thus low Young's modulus. For cell encapsulation applications, significant volume change of hydrogel under cell culture environment should be avoided. Therefore, the swelling behavior of hydrogel prepared under different pH was tested. The degree of swelling of the hydrogel prepared under pH = 7.8 was slightly lower (26.9 ± 1.1) compared with the hydrogels prepared under pH = 7.0 (36.8 ± 0.9) (Fig. 2D). The result was in agreement with the changing trends of Young's modulus, due to the high cross-linking density under pH = 7.8. We further tested the swelling volume ratio of hydrogel prepared under different pH (Fig. 2D), which decreased gradually with increasing pH. The swelling volume ratio of hydrogel was 1.71 ± 0.06 under pH = 7.4, indicating that the volume change of the hydrogel prepared under physiological pH is not obvious. These results demonstrate that the hydrogel is suitable for 3D cell encapsulation.

The effect of pH on surface texture of freeze-dried Dex-l-DTT hydrogels was characterized by using scanning electron microscopy (SEM) (Fig. 2E–G). For all the hydrogels prepared under

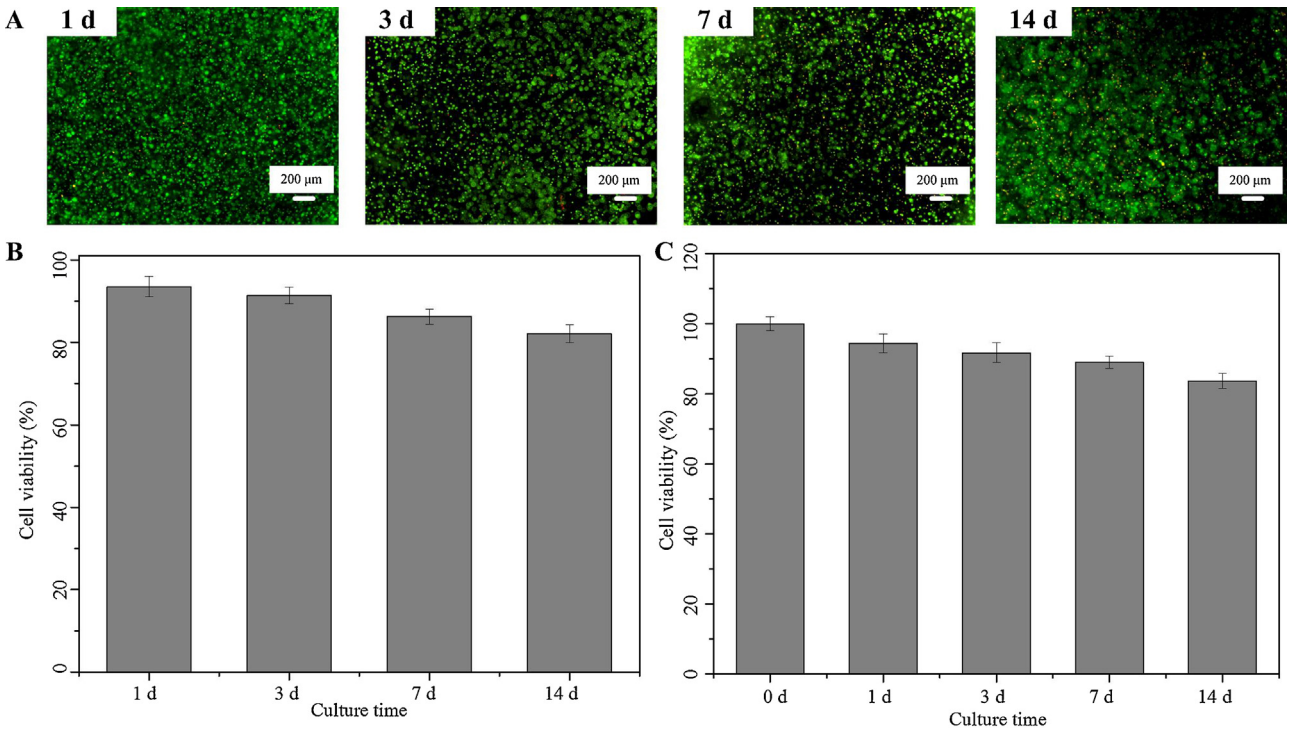

Fig. 6. Viability of NIH/3T3 fibroblasts encapsulated in Dex-l-DTT hydrogel. (A) Live/dead images of NIH/3T3 fibroblasts encapsulated in hydrogels for 1 d, 3 d, 7 d, and 14 d. A green fluorescence designates live cells, whereas a red fluorescence indicates dead cells. (B) The cell viability obtained from the fluorescent images. (C) Cell viability of encapsulated NIH/3T3 fibroblasts detected by MTT assay. Error ranges are standard deviations over $n = 4$ samples. (For interpretation of the references to color in this figure legend, the reader is referred to the web version of the article.)

different pH, their pores appeared to be interconnected, which could facilitate diffusion of molecules and oxygen, providing proper conditions for cell encapsulation. We observed that the pore size increased from 0.44 ± 0.03 μm to 14.2 ± 1.9 μm and 62.2 ± 14.9 μm when the pH decreased from 7.8 to 7.4 and 7.0. Besides, high pH condition gave more homogeneous pore size. These phenomena can be explained as that more activated function groups (methyl acrylate and thiol groups) participate in gelation process under high pH, contributing to the high cross-linking density, and thus smaller pores, and vice versa. These results demonstrate that the pore size can be tuned by changing pH condition for forming hydrogels, which may provide suitable in situ forming hydrogel system for different soft scaffold applications [52].

3.3. Cytotoxicity and 3D cell encapsulation

Cytocompatibility is critical for biomaterials used for 3D cell encapsulation [53]. To evaluate the cytotoxicity of the Dex-GMA polymer and DTT cross-linker, we performed 3-(4,5-dimethylthiazolyl-2)-2,5-diphenyltetrazolium bromide (MTT) assay by directly adding Dex-GMA or DTT into cell culture medium. Cell viability of NIH/3T3 fibroblasts and BMSCs under the action of Dex-GMA was independent on concentration and treatment time. The cell viability of both kinds of cells was as high as ~95% even under high concentration (2.0 mg/mL) and long treatment time (24 h) (Fig. 3A and C). When the treatment time was extended to 48 h, MTT value of NIH/3T3 fibroblasts under the action of Dex-GMA with different concentration increased to ~150%, which was similar to that without Dex-GMA, indicating that NIH/3T3 fibroblasts proliferated normally under the action of Dex-GMA (Fig. 3A). All these data indicate the excellent cytocompatibility of Dex-GMA polymer.

However, cell viability of NIH/3T3 fibroblasts and BMSCs under the action of DTT was as low as ~55% and ~50%, respectively, when the DTT concentration was in a range of 0.5–2.0 mg/mL under 24 h treatment time (Fig. 3B and D). When the treatment time was extended to 48 h, cell viability of both kinds of cells decreased gradually with the increase of DTT concentration. It indicates that cytotoxicity of DTT is notable under long treatment time. Similar results have also been reported in literature [12].

In fact, the in situ-forming Dex-l-DTT hydrogel ($R = 1$, pH = 7.4) with encapsulated cells could be formed within 5 min, which is a little longer than the gelation process without cells. Taking into account the fast gelation process and high reaction efficiency, there is not a large amount of DTT existing for such long treatment time in cell culture medium. Therefore, it is reasonable to detect the cytotoxicity of DTT in a short treatment time. When treatment time was 5 min, cell viability was as high as ~91% even under high DTT concentration (2.0 mg/mL). Moreover, the cell viability was high than 80% when treatment time was 10 and 15 min (Fig. 4). The results indicate that most of the cells could survive during the short in situ gelation process.

Cell encapsulation was performed to investigate the potential to use the Dex-l-DTT hydrogel as encapsulation matrices. The NIH/3T3 fibroblasts or BMSCs laden hydrogels were prepared by mixing cell suspension (3×10^6 cell/mL) with cell culture medium containing the Dex-GMA polymer and DTT cross-linker under physiological conditions (Fig. 5A). Following hydrogel formation, the cell-laden hydrogels were cultured under standard conditions, and cell viability was assessed using live/dead staining and MTT assay, separately. At the initial time of cultivation (0~24 h), the culture medium was changed every 6 h to remove the small amount of unreacted chemicals. After 24 h, the culture medium was refreshed every day to support cell growth. The live/dead staining was conducted at the time point of interest (1, 3, 7, and 14 d) and the images of fluorescence microscopy demonstrate that most of the cells encapsulated in the hydrogel matrix remain alive after 14 d

cultivation (Figs. 5B and 6A). Green fluorescence designates live cells, whereas red fluorescence indicates dead cells. Quantitative analysis of the images showed that there was a high viability of encapsulated BMSCs (81 ± 2%) and NIH/3T3 fibroblasts (91 ± 2%) at 3 d post-encapsulation. When the culture time was extended to 14 d, cell viability of encapsulated BMSCs (72 ± 1%) and NIH/3T3 fibroblasts (82 ± 2%) was still high (Figs. 5C and 6B). The MTT data indicated that although cell viability slightly decreased with the increase of culture time, there was a high viability of encapsulated BMSCs (72 ± 6%) and NIH/3T3 fibroblasts (83 ± 2%) at 14 d post-encapsulation (Figs. 5D and 6C), which was consistent with the results obtained by live/dead staining. These results clearly demonstrate the good cytocompatibility of the in situ-forming Dex-l-DTT hydrogel.

As one kind of adult stem cells, BMSCs can differentiate into osteoblasts under different conditions [54]. When cultured in osteogenic induction medium, BMSCs can differentiate into osteoblasts, and alkaline phosphatase (ALP) plays an important role during the calcified tissue formation process. As described in previously reported literatures, ALP expression of BMSC cultured in osteogenic induction medium increased at the initial culture time and then started to decrease after culturing for about 10–14 days [55,56]. To quantify the differentiation ability of BMSCs encapsulated in the Dex-l-DTT hydrogel, ALP activity was detected at day 1, 3, 5, 7, 9, and 14. ALP activity was very low at the initial culture time point (day 1) and significant increase was detected from day 3, reaching a peak at day 9, and then, the ALP activity decreased gradually (Fig. 5E), which was consistent with the previous report [55,56], demonstrating the osteogenesis process. As a contrast, the increase of ALP expression of BMSC cultured in normal medium (control group) is not significant. The results indicate that the BMSCs encapsulated in the Dex-l-DTT hydrogels could not only survive, but also maintain their differentiation ability.

4. Conclusions

In summary, this work presents the thiol-Michael click reaction to synthesize in situ-forming dextran-based Dex-l-DTT hydrogels for 3D cell encapsulation. The gelation process, mechanical properties, degree of swelling, swelling volume ratio and morphology of surface texture of the hydrogel can be easily tuned by adjusting the pH of the system ranging from 7.0 to 7.8. BMSCs and NIH/3T3 fibroblasts were successfully encapsulated into the hydrogel with maintained high viability, demonstrating the good cytocompatibility of the hydrogel. ALP activity assay suggested that encapsulated BMSCs can not only remain viability but also maintain differentiation potential. The combination of tunable properties and good cytocompatibility demonstrates the potential of the Dex-l-DTT hydrogels to be used as 3D scaffold for cell encapsulation.

Acknowledgements

This research was supported by National Natural Science Foundation of China (Grants 51173144 and 51073127), the Research Fund for the Doctoral Program of Higher Education of China, Scientific Research Foundation for the Returned Overseas Chinese Scholars, State Education Ministry, the Fundamental Research Funds for the Central Universities, International Science & Technology Cooperation Program Supported by Ministry of Science and Technology of China and Shaanxi Province (2013KW14-02), Key Innovational Research Team Program Supported by Shaanxi Province (2013KCT-05). F.X. was supported by the Chinese National Science Foundation (11372243), International Science & Technology Cooperation Program of China (2013DFG02930).

Appendix A. Supplementary data

Supplementary material related to this article can be found, in the online version, at http://dx.doi.org/10.1016/j.colsurfb.2015.02.005.

References

[1] M.W. Tibbitt, K.S. Anseth, Hydrogels as extracellular matrix mimics for 3D cell culture, Biotechnol. Bioeng. 103 (2009) 655–663.
[2] K. Chawla, T.B. Yu, S.W. Liao, Z. Guan, Biodegradable and biocompatible synthetic saccharide—peptide hydrogels for three-dimensional stem cell culture, Biomacromolecules 12 (2011) 560–567.
[3] K.M. Charoen, B. Fallica, Y.L. Colson, M.H. Zaman, M.W. Grinstaff, Embedded multicellular spheroids as a biomimetic 3D cancer model for evaluating drug and drug-device combinations, Biomaterials 35 (2014) 2264–2271.
[4] D. Loessner, K.S. Stok, M.P. Lutolf, D.W. Hutmacher, J.A. Clements, S.C. Rizzi, Bioengineered 3D platform to explore cell–ECM interactions and drug resistance of epithelial ovarian cancer cells, Biomaterials 31 (2010) 8494–8506.
[5] P.C. Tseng, T.H. Young, T.M. Wang, H.W. Peng, S.M. Hou, M.L. Yen, Spontaneous osteogenesis of MSCs cultured on 3D microcarriers through alteration of cytoskeletal tension, Biomaterials 33 (2012) 556–564.
[6] S.K. Oh, A.K. Chen, Y. Mok, X. Chen, U.M. Lim, A. Chin, A.B. Choo, S. Reuveny, Long-term microcarrier suspension cultures of human embryonic stem cells, Stem Cell Res. 2 (2009) 219–230.
[7] A.M. Fernandes, T.G. Fernandes, M.M. Diogo, C.L. da Silva, D. Henrique, J.M. Cabral, Mouse embryonic stem cell expansion in a microcarrier-based stirred culture system, J. Biotechnol. 132 (2007) 227–236.
[8] N. Di Maggio, E. Piccinini, M. Jaworski, A. Trumpp, D.J. Wendt, I. Martin, Toward modeling the bone marrow niche using scaffold-based 3D culture systems, Biomaterials 32 (2011) 321–329.
[9] S.V. Bhujbal, P. de Vos, S.P. Niclou, Drug and cell encapsulation: alternative delivery options for the treatment of malignant brain tumors, Adv. Drug Delivery Rev. 67-68 (2014) 142–153.
[10] L.U. Wahlberg, G. Lind, P.M. Almqvist, P. Kusk, J. Tornoe, B. Juliusson, M. Soderman, E. Sellden, A. Seiger, M. Eriksdotter-Jonhagen, B. Linderoth, Targeted delivery of nerve growth factor via encapsulated cell biodelivery in Alzheimer disease: a technology platform for restorative neurosurgery, J. Neurosurg. 117 (2012) 340–347.
[11] M.J. Oh, T.K. Ryu, S.W. Choi, Hollow polydimethylsiloxane beads with a porous structure for cell encapsulation, Macromol. Rapid Commun. 34 (2013) 1728–1733.
[12] G.D. Nicodemus, S.J. Bryant, Cell encapsulation in biodegradable hydrogels for tissue engineering applications, Tissue Eng. Part B 14 (2008) 149–165.
[13] S. Gerecht, S.A. Townsend, H. Pressler, H. Zhu, C.L. Nijst, J.P. Bruggeman, J.W. Nichol, R. Langer, A porous photocurable elastomer for cell encapsulation and culture, Biomaterials 28 (2007) 4826–4835.
[14] D.Q. Wu, Y.X. Sun, X.D. Xu, S.X. Cheng, X.Z. Zhang, R.X. Zhuo, Biodegradable and pH-sensitive hydrogels for cell encapsulation and controlled drug release, Biomacromolecules 9 (2008) 1155–1162.
[15] Y.M. Chen, M. Tanaka, J.P. Gong, K. Yasuda, S. Yamamoto, M. Shimomura, Y. Osada, Platelet adhesion to human umbilical vein endothelial cells cultured on anionic hydrogel scaffolds, Biomaterials 28 (2007) 1752–1760.
[16] J.F. Liu, Y.M. Chen, J.J. Yang, T. Kurokawa, A. Kakugo, K. Yamamoto, J.P. Gong, Dynamic behavior and spontaneous differentiation of mouse embryoid bodies on hydrogel substrates of different surface charge and chemical structures, Tissue Eng. Part A 17 (2011) 2343–2357.
[17] K.J.R. Lewis, K.S. Anseth, Hydrogel scaffolds to study cell biology in four dimensions, MRS Bull. 38 (2013) 260–268.
[18] F. Lin, J. Yu, W. Tang, J. Zheng, A. Defante, K. Guo, C. Wesdemiotis, M.L. Becker, Peptide-functionalized oxime hydrogels with tunable mechanical properties and gelation behavior, Biomacromolecules 14 (2013) 3749–3758.
[19] H.K. Kleinman, G.R. Martin, Matrigel: basement membrane matrix with biological activity, Semin. Cancer Biol. 15 (2005) 378–386.
[20] L. Bessea, B. Coulomb, C. Lebreton-Decoster, M.M. Giraud-Guille, Production of ordered collagen matrices for three-dimensional cell culture, Biomaterials 23 (2002) 27–36.
[21] C.S. Szot, C.F. Buchanan, J.W. Freeman, M.N. Rylander, 3D in vitro bioengineered tumors based on collagen I hydrogels, Biomaterials 32 (2011) 7905–7912.
[22] S.M. Willerth, K.J. Arendas, D.I. Gottlieb, S.E. Sakiyama-Elbert, Optimization of fibrin scaffolds for differentiation of murine embryonic stem cells into neural lineage cells, Biomaterials 27 (2006) 5990–6003.
[23] G.N. Grover, J. Lam, T.H. Nguyen, T. Segura, H.D. Maynard, Biocompatible hydrogels by oxime Click chemistry, Biomacromolecules 13 (2012) 3013–3017.
[24] Y.B. Wu, L. Wang, B.L. Guo, P.X. Ma, Injectable biodegradable hydrogels and microgels based on methacrylated poly(ethylene glycol)-co-poly(glycerol sebacate) multi-block copolymers: synthesis, characterization, and cell encapsulation, J. Mater. Chem. B 2 (2014) 3674–3685.
[25] A. Terella, P. Mariner, N. Brown, K. Anseth, S.O. Streubel, Repair of a calvarial defect with biofactor and stem cell-embedded polyethylene glycol scaffold, Facial Plast. Surg. 12 (2010) 166–171.
[26] A. Metters, J. Hubbell, Network formation and degradation behavior of hydrogels formed by Michael-type addition reactions, Biomacromolecules 6 (2005) 290–301.

[27] H. Tseng, D.S. Puperi, E.J. Kim, S. Ayoub, J.V. Shah, M.L. Cuchiara, J.L. West, K.J. Grande-Allen, Anisotropic poly(ethylene glycol)/polycaprolactone hydrogel-fiber composites for heart valve tissue engineering, Tissue Eng. Part A 20 (2014) 2634–2645.
[28] S.H. Cho, S.H. Oh, J.H. Lee, Fabrication and characterization of porous alginate/polyvinyl alcohol hybrid scaffolds for 3D cell culture, J. Biomater. Sci. Polym. Ed. 16 (2005) 933–947.
[29] T.T. Gan, Y.J. Zhang, Y. Guan, In situ gelation of P(NIPAM-HEMA) microgel dispersion and its applications as injectable 3D cell scaffold, Biomacromolecules 10 (2009) 1410–1415.
[30] M.A. Azagarsamy, K.S. Anseth, Bioorthogonal click chemistry: an indispensable tool to create multifaceted cell culture scaffolds, ACS Macro. Lett. 2 (2013) 5–9.
[31] Y.M. Chen, R. Ogawa, A. Kakugo, Y. Osada, J.P. Gong, Dynamic cell behavior on synthetic hydrogels with different charge densities, Soft Matter. 5 (2009) 1804–1811.
[32] Y.M. Chen, N. Shiraishi, H. Satokawa, A. Kakugo, T. Narita, J.P. Gong, Y. Osada, K. Yamamoto, J. Ando, Cultivation of endothelial cells on adhesive protein-free synthetic polymer gels, Biomaterials 26 (2005) 4588–4596.
[33] Y.M. Chen, Z.Q. Liu, Z.H. Feng, F. Xu, J.K. Liu, Adhesive protein-free synthetic hydrogels for retinal pigment epithelium cell culture with low ROS level, J. Biomed. Mater. Res. Part A 102 (2014) 2258–2267.
[34] J.A. Burdick, G.D. Prestwich, Hyaluronic acid hydrogels for biomedical applications, Adv. Mater. 23 (2011) H41–H56.
[35] V. Crescenzi, L. Cornelio, C. Di Meo, S. Nardecchia, R. Lamanna, Novel hydrogels via click chemistry: synthesis and potential biomedical applications, Biomacromolecules 8 (2007) 1844–1850.
[36] C.J. Martinez, J.W. Kim, C. Ye, I. Ortiz, A.C. Rowat, M. Marquez, D. Weitz, A microfluidic approach to encapsulate living cells in uniform alginate hydrogel microparticles, Macromol. Biosci. 12 (2012) 946–951.
[37] C. Hiemstra, L.J. van der Aa, Z.Y. Zhong, P.J. Dijkstra, J. Feijen, Novel in situ forming, degradable dextran hydrogels by Michael addition chemistry: synthesis, rheology, and degradation, Macromolecules 40 (2007) 1165–1173.
[38] C. Hiemstra, L.J. van der Aa, Z.Y. Zhong, P.J. Dijkstra, J. Feijen, Rapidly in situ-forming degradable hydrogels from dextran thiols through Michael addition, Biomacromolecules 8 (2007) 1548–1556.
[39] Z. Wei, J.H. Yang, X.J. Du, F. Xu, M. Zrinyi, Y. Osada, F. Li, Y.M. Chen, Dextran-based self-healing hydrogels formed by reversible Diels–Alder reaction under physiological conditions, Macromol. Rapid Commun. 34 (2013) 1464–1470.
[40] T.R. Hoare, D.S. Kohane, Hydrogels in drug delivery: progress and challenges, Polymer 49 (2008) 1993–2007.
[41] S.J. de Jong, B. van Eerdenbrugh, C.F. van Nostrum, J.J. Kettenes-van den Bosch, W.E. Hennink, Physically crosslinked dextran hydrogels by stereocomplex formation of lactic acid oligomers: degradation and protein release behavior, J. Control. Release 71 (2001) 261–275.
[42] Y. Wang, A. Brunsen, U. Jonas, J. Dostalek, W. Knoll, Prostate specific antigen biosensor based on long range surface plasmon-enhanced fluorescence spectroscopy and dextran hydrogel binding matrix, Anal. Chem. 81 (2009) 9625–9632.
[43] Y. Fan, C. Deng, R. Cheng, F. Meng, Z. Zhong, In situ forming hydrogels via catalyst-free and bioorthogonal tetrazole-alkene photo-click chemistry, Biomacromolecules 14 (2013) 2814–2821.
[44] R. Zhang, M. Xue, J. Yang, T. Tan, A novel injectable and in situ crosslinked hydrogel based on hyaluronic acid and α,β-polyaspartylhydrazide, J. Appl. Polym. Sci. 125 (2012) 1116–1126.
[45] J.D. McCall, K.S. Anseth, Thiol-ene photopolymerizations provide a facile method to encapsulate proteins and maintain their bioactivity, Biomacromolecules 13 (2012) 2410–2417.
[46] X. Sui, L. van Ingen, M.A. Hempenius, G.J. Vancso, Preparation of a rapidly forming poly(ferrocenylsilane)-poly(ethylene glycol)-based hydrogel by a thiol-Michael addition click reaction, Macromol. Rapid Commun. 31 (2010) 2059–2063.
[47] Y. Yu, Y. Chau, One-step click method for generating vinyl sulfone groups on hydroxyl-containing water-soluble polymers, Biomacromolecules 13 (2012) 937–942.
[48] W.N.E. Vandijkwolthuis, O. Franssen, H. Talsma, M.J. Vansteenbergen, J.J.K. Vandenbosch, W.E. Hennink, Synthesis, characterization, and polymerization of glycidyl methacrylate derivatized dextran, Macromolecules 28 (1995) 6317–6322.
[49] M. Soleimani, S. Nadri, A protocol for isolation and culture of mesenchymal stem cells from mouse bone marrow, Nat. Protoc. 4 (2009) 102–106.
[50] L. Zheng, F. Yang, H. Shen, X. Hu, C. Mochizuki, M. Sato, S. Wang, Y. Zhang, The effect of composition of calcium phosphate composite scaffolds on the formation of tooth tissue from human dental pulp stem cells, Biomaterials 32 (2011) 7053–7059.
[51] D.L. Alge, M.A. Azagarsamy, D.F. Donohue, K.S. Anseth, Synthetically tractable click hydrogels for three-dimensional cell culture formed using tetrazine-norbornene chemistry, Biomacromolecules 14 (2013) 949–953.
[52] Y. Dong, A.O. Saeed, W. Hassan, C. Keigher, Y. Zheng, H. Tai, A. Pandit, W. Wang, One-step preparation of thiol-ene clickable PEG-based thermoresponsive hyperbranched copolymer for in situ crosslinking hybrid hydrogel, Macromol. Rapid Commun. 2012 (2011) 120–126.
[53] B. Yang, Y.L. Zhang, X.Y. Zhang, L. Tao, S.X. Li, Y. Wei, Facilely prepared inexpensive and biocompatible self-healing hydrogel: a new injectable cell therapy carrier, Polym. Chem. 3 (2012) 3235–3238.
[54] H. Motaln, C. Schichor, T.T. Lah, Human mesenchymal stem cells and their use in cell-based therapies, Cancer Am. Cancer 116 (2010) 2519–2530.
[55] M.F. Pittenger, A.M. Mackay, S.C. Beck, R.K. Jaiswal, R. Douglas, J.D. Mosca, M.A. Moorman, D.W. Simonetti, S. Craig, D.R. Marshak, Multilineage potential of adult human mesenchymal stem cells, Science 284 (1999) 143–147.
[56] Y. Wang, W. Peng, X. Liu, M. Zhu, T. Sun, Q. Peng, Y. Zeng, B. Feng, W. Zhi, J. Weng, J. Wang, Study of bilineage differentiation of human-bone-marrow-derived mesenchymal stem cells in oxidized sodium alginate/N-succinyl chitosan hydrogels and synergistic effects of RGD modification and low-intensity pulsed ultrasound, Acta Biomater. 10 (2014) 2518–2528.